

# Microscopic flux density of small and dendritic flux jumps in MgB<sub>2</sub> thin films

Jae-Yeap Lee<sup>1</sup>, Eun-Mi Choi<sup>1</sup>, Hyun-Sook Lee<sup>1</sup>, Hu-Jong Lee<sup>1</sup>,  
Sung-Ik Lee<sup>2</sup>, Å A F Olsen<sup>3</sup>, D V Shantsev<sup>3</sup> and T H Johansen<sup>3</sup>

<sup>1</sup> National Creative Research Initiative Center for Superconductivity, Department of Physics, Pohang University of Science and Technology, Pohang 790-784, Republic of Korea

<sup>2</sup> National Creative Research Initiative Center for Superconductivity, Department of Physics, Sogang University, Seoul, Korea

<sup>3</sup> Department of Physics, University of Oslo, PO Box 1048 Blindern, N-0316 Oslo, Norway

E-mail: [silee77@sogang.ac.kr](mailto:silee77@sogang.ac.kr)

Received 6 July 2008, in final form 5 August 2008

Published 21 August 2008

Online at [stacks.iop.org/SUST/21/105021](http://stacks.iop.org/SUST/21/105021)

## Abstract

In contrast to the detailed study on macroscopic vortex avalanches, the development of microscopic small flux jumps and dendritic branches during the growth of an avalanche in a MgB<sub>2</sub> thin film with changing temperature and magnetic field is not well studied. Our study of the two phenomena shows that the number and the size of the small flux jumps and the maximum flux density critically depend on the width of the rectangular thin film with dimensions 3 mm × width for film width ranging from 0.2 to 1.6 mm. We also found that when the ratio between the maximum field density and the applied flux was below 1, dendrites do not exist.

## 1. Introduction

When a magnetic field penetrates into thin films of type-II superconductors, vortex avalanches take place in some materials. This phenomenon, often seen as a sudden formation of dendritic flux structures, is observed in Nb, Nb alloys, and YBa<sub>2</sub>Cu<sub>3</sub>O<sub>x</sub> thin films when a pulsed laser is applied to trigger avalanches [1–7]. Most previous works have been focused on MgB<sub>2</sub> thin films, where the richness and the intriguing features of this phenomenon have been investigated both experimentally and theoretically [8–15]. This type of vortex avalanche is claimed to originate from a thermo-magnetic instability as a result of the competition between thermal and magnetic diffusivity. When thermal diffusion is the slower of the two, the superconducting film is unstable, and dendritic avalanches appear [11–15]. Dendritic vortex avalanches in MgB<sub>2</sub> thin films appear below a certain temperature ( $T < 10$  K) and in a magnetic field ranging between a lower and upper threshold value [15, 16]. These avalanches, which lower the critical current density, are most detrimental to the use of superconducting thin films for practical applications. Two methods have successfully been designed to suppress the phenomenon: (i) depositing a metal layer on the MgB<sub>2</sub> film to dissipate the heat generated from the moving vortices

which reduce the thermo-magnetic instability [10, 17], and (ii) changing the geometry of the thin films. Once the width of the film gets smaller than a certain value, the avalanches disappear. The region between the lower and upper threshold fields where the vortex avalanches appear reduces as the width of the sample is decreased [15, 18]. Under conditions where MgB<sub>2</sub> films show avalanche activity, one finds that the flux jumps are consistently classified into two different categories [14, 19, 20]. One is an avalanche having distinct dendritic branches that extend deep into the sample area. The other is small flux jumps, which occur as a part of the background flux penetration near the edge of the sample. Whereas the geometry dependence of the dendritic branch formation has been well documented, very little is known about the small flux jumps and how their formation depends on the sample's dimensions. Thus, in this study, we carefully examined the small flux jump behavior by taking magneto-optical imaging (MOI) measurements on a set of different-sized MgB<sub>2</sub> rectangular films, and we report here the results of the small flux jump behavior. From this measurement, we found that the small flux jumps and the maximum flux density in dendritic branches are also affected by the sample's width.

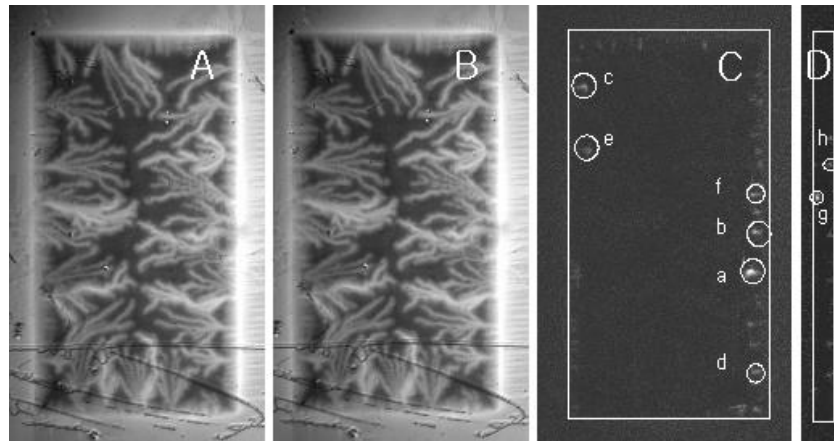


**Figure 1.** Magneto-optical images of flux penetration at 19.9 mT (A) and 20.2 mT (B). Subtraction of the two images reveals the small flux jumps in the  $w = 1.6$  mm sample (C). The result obtained by using the same method for a  $w = 0.2$  mm strip is shown in (D).

## 2. Experiments and discussion

MgB<sub>2</sub> thin films were fabricated by using a two-step method with a pulsed laser deposition system [21]. Throughout the process, the samples were never exposed to air, in order to prevent contamination with carbon or oxygen. At 39 K, a sharp superconducting transition was confirmed from the magnetization-curve measurements. Scanning electron microscopy results show that the thin films were *c*-axis oriented and had a thicknesses of 300 nm. Electron probe microanalysis (EPMA) showed that the thin films were carbon free within the resolution limit (0.01%) [17]. By using photolithography, we patterned on one substrate eight sets of films with rectangular shapes of 3 mm ×  $w$ , where the width  $w = 1.6, 1.2, 0.9, 0.7, 0.5, 0.4, 0.3,$  and 0.2 mm. We obtained magneto-optical images by using a standard MOI setup at  $T = 3.8$  K. A ferrite garnet sensor film with a strong Faraday effect revealed the magnetic flux distribution over the sample's area as an image of brightness distribution when viewed through a polarizing microscope with crossed polarizers [22].

With MOI, the small flux jumps are seen near the flux front as it progressively penetrates the MgB<sub>2</sub> thin film. Since their size is very small, clear pictures of individual jumps are best obtained by subtracting two images recorded with a small difference in the applied magnetic field. Shown in figure 1 is one example, where figures 1(C) and (D) were obtained by subtracting the image taken at 19.9 mT from that taken at 20.2 mT. The small flux jumps are seen as bright small areas close to the edge. It is readily seen that there are more small flux jumps in the 1.6 mm wide film than in the most narrow 0.2 mm wide film. To quantify the size of the small flux jump, we determined the total number of vortices in the largest individual jumps marked from a to g in figures 1(C) and (D). The result is shown in figure 2. In the 1.6 mm wide film, many small flux jumps involve  $\sim 10^4$  vortices, which is about one order of magnitude larger than that for a narrow film. Thus, the maximum jump size shows clear sample-size dependence. In this study, we also measured the maximum flux density in each dendritic branch for different sample widths. All dendritic branches formed for applied fields between 14.1

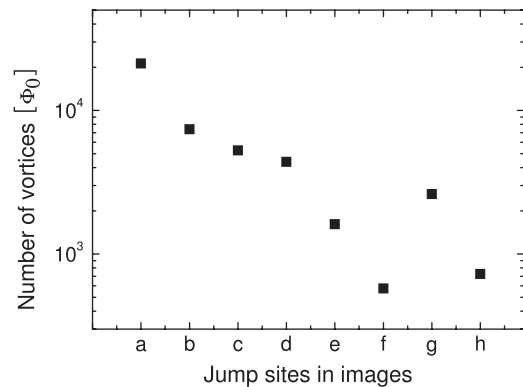


**Figure 2.** Size of the small flux jumps in the  $w = 1.6$  and 0.2 mm samples. (a)–(f) are from the wide strip, and (g), (h) are from the narrow strip.

and 15.3 mT for films with widths from 0.2 to 1.6 mm are shown in figure 3. The exact position of the maximum flux density, i.e., the position of largest brightness, is indicated in the figure by open rings. Shown in figure 4 are the data of the maximum flux density as a function of the sample width. From  $w = 1.6$  mm down to  $w = 0.4$  mm, the maximum flux density was almost constant, but with a very slow decrease at smaller widths. Below  $w = 0.3$  mm, however, the maximum flux density decreases very rapidly, and the maximum flux density of the  $w = 0.2$  mm sample had the lowest value among our eight samples. The difference in the maximum flux density between the  $w = 0.2$  mm and 1.6 mm samples is 7 mT.

To show the relation between the maximum flux density and the applied magnetic field where the dendrites were formed, we draw in figure 5 the maximum flux density/applied field ratio for all the films. The line drawn in the graph is a fit to the experimental data points obtained by using a simple functional form:

$$y(x) = 1.61 - 1.49e^{\left[\frac{x}{0.148}\right]}. \quad (1)$$

In this formula,  $x$  is the sample width and  $y$  is the local maximum field. For all eight samples, the maximum flux

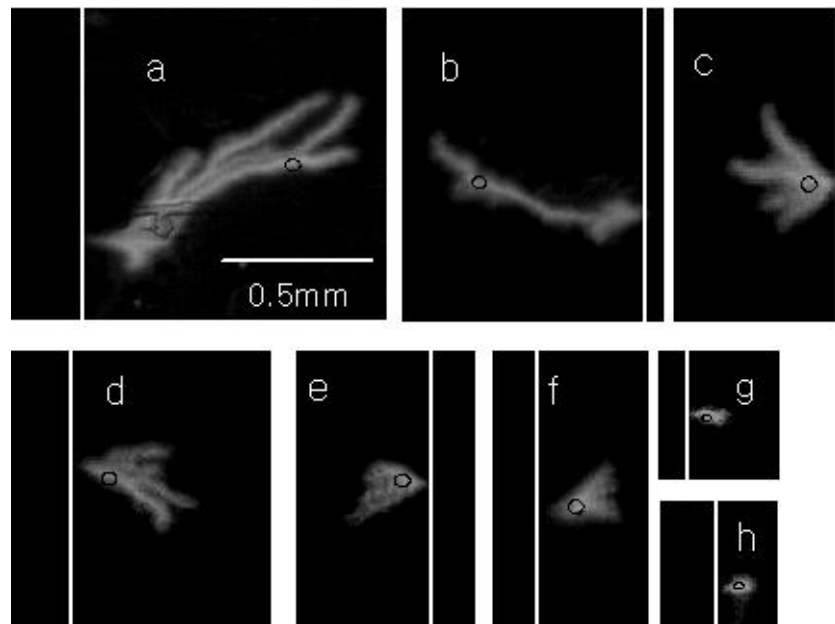


**Figure 3.** Magneto-optical images of flux dendrites formed as the applied field was increased from 14.1 to 15.3 mT. The panels (a)–(h) show the eight samples with widths from 1.6 to 0.2 mm. The open rings indicate the brightest parts of each dendrite, and the white line is the film's edge.

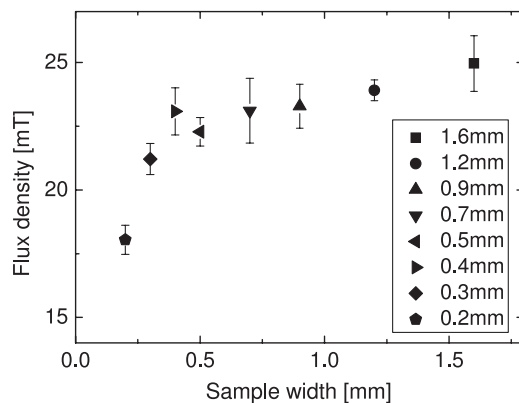


**Figure 4.** The maximum flux density obtained from sample widths ranging from 0.2 to 1.6 mm.

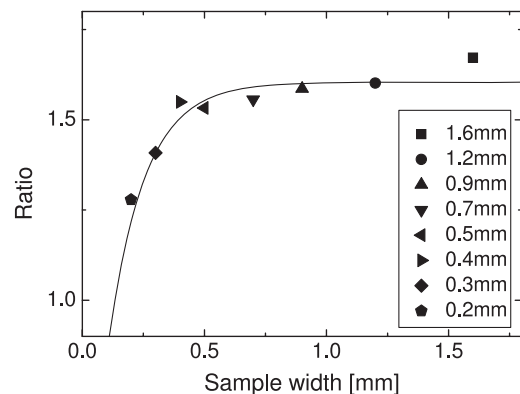


**Figure 5.** The ratio between the maximum flux density and the applied magnetic field as a function of the sample width.

density/applied field ratio was larger than 1, with the smallest value of 1.3 found for the  $w = 0.2$  mm film. In a previous investigation [13], we found that dendrites formed in such  $\text{MgB}_2$  films only for  $w < 0.164$  mm. Interestingly, the fitted curve extrapolates to 1 for a value of  $w$  very close to the lower limit for the dendrite formation. This suggests that the maximum flux density is always larger than the applied field at which a dendrite forms.

### 3. Conclusions

In this paper, the relations between the sample geometry and the small flux jump and the maximum flux density were studied based on detailed measurements using a magneto-optical imaging technique. As the  $\text{MgB}_2$  sample becomes narrower, the small flux jumps occurring in the background of large-scale

dendritic flux jumps become increasingly suppressed. From an analysis, we find that the maximum flux density/applied field ratio approaches 1 when the sample width shrinks to the limiting value for the formation of dendritic flux avalanches. The above two phenomena are closely related to the demagnetization effect. The gradient of magnetic flux density from edge to inside the film is large for a film with larger width. In this case, a thin film feels stronger magnetic pressure and the magnetic diffusivity is weaker as the film is narrower. From these result, we can suppose that a narrow film has more stability than a wider one and this is consistent with the thermo-magnetic model.

### Acknowledgments

This work was supported by the Center of Superconductivity from the program of Acceleration Research of MOST/KOSEF

of Korea, special fund from Sogang University, and the Research Council of Norway.

## References

- [1] Duran C A, Gammel P L, Miller R E and Bishop D J 1995 *Phys. Rev. B* **52** 75
- [2] Rudnev I A, Antonenko S V, Shantsev D V, Johansen T H and Primenko A E 2003 *Cryogenics* **43** 663
- [3] Wimbush S C, Holzapfel B and Jooss Ch 2004 *J. Appl. Phys.* **96** 3589
- [4] Rudnev I A, Shantsev D V, Johansen T H and Primenko A E 2005 *Appl. Phys. Lett.* **87** 042502
- [5] Wertheimer M R and Gilchrist J de G 1967 *J. Phys. Chem. Solids* **28** 2509
- [6] Leiderer P, Boneberg J, Brüll P, Bujok V and Herminghaus S 1993 *Phys. Rev. Lett.* **71** 2646
- [7] Kang W N, Jung C U, Kim Kijoon H P, Park M-S, Lee S Y, Kim H-J, Choi E-M, Kim K H, Kim M-S and Lee S-I 2001 *Appl. Phys. Lett.* **79** 982
- [8] Zhao Z W, Li S L, Ni Y M, Yang H P, Liu Z Y, Wen H H, Kang W N, Kim H J, Choi E M and Lee S I 2002 *Phys. Rev. B* **65** 064512
- [9] Johansen T H, Baziljevich M, Shantsev D V, Goa P E, Galperin Y M, Kang W N, Kim H J, Choi E M, Kim M-S and Lee S I 2002 *Europhys. Lett.* **5** 599
- [10] Choi E-M, Lee H-S, Kim H-J, Lee S-I, Kim H-J and Kang W N 2004 *Appl. Phys. Lett.* **84** 82
- [11] Rakhmanov A L, Shantsev D V, Galperin Y M and Johansen T H 2004 *Phys. Rev. B* **70** 224502
- [12] Aranson I, Gurevich A, Welling M, Wijngaarden R, Vlasko-Vlasov V, Vinokur V and Welp U 2005 *Phys. Rev. Lett.* **94** 037002
- [13] Denisov D V, Rakhmanov A L, Shantsev D V, Galperin Y M and Johansen T H 2006 *Phys. Rev. B* **73** 014512
- [14] Shantsev D V, Bobyl A V, Galperin Y M, Johansen T H and Lee S I 2005 *Phys. Rev. B* **72** 024541
- [15] Denisov D V, Shantsev D V, Galperin Y M, Choi E-M, Lee H-S, Lee S-I, Bobyl A V, Goa P E, Olsen A A F and Johansen T H 2006 *Phys. Rev. Lett.* **97** 077002
- [16] Choi E-M, Lee H-S, Lee J-Y, Lee S-I, Olsen A A F, Yurchenko V V, Shantsev D V, Johansen T H, Kim H-J and Cho M-H 2007 *Appl. Phys. Lett.* **91** 1
- [17] Choi E-M, Lee H-S, Kim H J, Kang B, Lee S-I, Olsen A A F, Shantsev D V and Johansen T H 2005 *Appl. Phys. Lett.* **87** 152501
- [18] Choi E-M, Lee H-S, Lee S-I, Olsen A A F, Shantsev D V and Johansen T H 2006 *J. Korean Phys. Soc.* **48** 1044–7
- [19] Bobyl A V, Shantsev D V, Galperin Y M, Olsen A A F, Johansen T H, Kang W N and Lee S I 2004 *Physica C* **408–410** 508–9
- [20] Barkov F L, Shantsev D V, Johansen T H, Goa P E, Kang W N, Kim H J, Choi E M and Lee S I 2003 *Phys. Rev. B* **67** 064513
- [21] Kang W N, Kim H-J, Choi E-M, Jung C U and Lee S-I 2001 *Science* **292** 1521
- [22] Johansen T H, Baziljevich M, Bratsberg H, Galperin Y, Lindelof P E, Shen Y and Vase P 1996 *Phys. Rev. B* **54** 16264